In Situ Grown Titania Composition for Optimal Performance and Durability of Nafion® Fuel Cell Membranes

Yatin Patil, Sunil Kulkarni, Kenneth A. Mauritz

School of Polymers and High performance Materials, University of Southern Mississippi, Hattiesburg, Mississippi 39406-0001

Received 4 August 2009; accepted 27 September 2009
DOI 10.1002/app.31500
Published online 21 March 2011 in Wiley Online Library (wileyonlinelibrary.com).

ABSTRACT: Nafion® membranes were modified via *in situ*, catalyzed sol–gel reactions of titanium isopropoxide to form titania particles in the polar acid domains. FTIR spectroscopy showed successful intraparticle chemical bond formation with incomplete condensation of TiOH groups. Although such modification can lower membrane fuel cell performance, this study was aimed at reducing membrane degradation without significantly altering performance in the sense of material optimization. These incorporated particles did not change membrane equivalent weight and the water uptake was similar to that of the unmodified Nafion® membrane. Membrane dimensional stability, mechanical properties, and ability to withstand contractile stresses associated with humidity change at 80°C and 100% RH were improved. An open circuit voltage (OCV) accelerated degradation test showed the titania modification held voltage better than the unmodified membrane. Performance deterioration of Nafion® after the OCV test was much higher than that of the modified membrane and the fluoride emission of the latter was lower. The degraded Nafion® membrane failed when subjected to creep, whereas the modified membrane remained intact with significantly low deformation. This inorganic modification offers a simple way to enhance membrane durability by reducing both physical and chemical degradation. © 2011 Wiley Periodicals, Inc. J Appl Polym Sci 121: 2344–2353, 2011

Key words: gas permeation; inorganic materials; ionomers; mechanical properties; membranes

INTRODUCTION

Fuel crossover in a polymer electrolyte membrane (PEM) fuel cell is a major cause for membrane failure. The benchmark PEM for fuel cells is Nafion® (E.I. DuPont) poly(perfluorosulfonic acid) that has a tetrafluoroethylene backbone and perfluoroalkylether side chains terminated by sulfonic acid groups.[1] In most situations, abrupt fuel cell failures occur in the membrane due to massive fuel crossover owing to pinholes and crack formation attributed to the coupled effects of physical and chemical degradation.[2,3]

Physical degradation of Nafion® membranes can be attributed to poor dimensional stability affected by relative humidity (RH) changes. Dimensional change due to an increase in humidity from 0 to 100% RH at fuel cell operating temperatures can be as high as 15%.[4] Different degrees of hydration are affected by humidity and temperature variations during fuel cell operations due to conditions of start-stop and changes in current density.[5] Water activity gradients across mechanically constrained membrane electrode assemblies (MEA) can cause differential swelling that generates internal stresses resulting in membrane deformation. Poor dimensional stability not only weakens membranes but also creates facile pathways for fuel crossover to form hydrogen peroxide, which is formed via incomplete reduction (two electrons) of oxygen on the catalyst surface.[6] Various studies support the crossover of both hydrogen and oxygen towards opposite electrodes as being responsible for membrane degradation.[7–10] Chemical degradation of Nafion® involves the attack of $^{\bullet}OH$ radicals that are generated from peroxide decomposition in the fuel cell environment.[11] It was proposed that the chemical attack occurs at the —COOH groups at the chain ends[12] although recent investigations of Schiraldi and coworkers demonstrated that attack also takes place, but at a lower rate, at the two ether oxygen atoms in the side chains.[13] In later versions, complete fluorination of Nafion® end groups does not stop

Correspondence to: K. A. Mauritz (kenneth.mauritz@usm.edu).

Contract grant sponsor: Department of Energy (US Department of Energy—Office of Energy Efficiency and Renewable Energy); contract grant number: DE-FG36-08GO88106.

degradation indicating that there are weak links elsewhere in the polymer.[14]

Physical and chemical degradation are synergistic, and the root cause is poor mechanical and gas barrier properties where hydrated interconnected ionic clusters provide paths of least resistance to gas diffusion.[15] After hydration, the membrane structure expands creating easy pathways for fuel gas to migrate to opposite electrodes.[16] Water-swollen regions of low mechanical modulus adjacent to drier regions of higher modulus could be loci of membrane failure owing to differential swelling stresses. During fuel cell operation, these regions continuously weaken due to reduced ductility and reduced molecular weight by chemical attack to form larger defects. The situation is analogous to an environmental stress crack resistance test wherein the reactive environment in this case contains $^{\bullet}OH$ radicals and the membrane is stretched due to humidity changes. This degradation process will continue until the weak regions eventually form pinholes resulting in ultimate failure. Thus, if fuel crossover can be reduced, the membrane will be less subjected to the reactive environment and last longer.

In concept, fuel crossover can be reduced by an effective concentration of nanoscopic particles that obstruct gas diffusion pathways. Furthermore, if these particles are slightly interconnected through metal oxide bonds, they would be a load-bearing network so that both mechanical and chemical degradation are limited. Nano-scale interpenetrating reinforcements will provide dimensional stability against humidity changes. Mauritz and Hassan reported studies of the incorporation of metal oxide and organically modified silicate nanoparticles in Nafion® by *in situ* sol–gel processes.[17]

The silicate precursor tetraethylorthosilicate (TEOS) and organically modified silicate nanoparticle precursors consisting of various organoalkoxysilanes were shown using SAXS to polymerize inside the hydrophilic domains of Nafion®.[18] Our previous work involving formation of Nafion®—*in situ* grown titania showed that such networks significantly reduce membrane degradation and improved mechanical and barrier properties that resist physical and chemical stresses.[19]

Here, after subjecting it to accelerated degradation conditions, the composite membrane's fuel cell performance was unchanged, whereas that of the unmodified Nafion® membrane deteriorated severely due to degradation. Although the inorganic sol–gel modification retarded membrane degradation, it resulted in reduced initial fuel cell performance due to decrease in proton conductivity. It is reasonable to think that the volume occupied by the nanoscopic particle networks in the ionic clusters decreased water uptake, restricted macromolecular mobility, and increased tortuosity all of which can influence proton migration. To overcome these problems, the network volume needs to be reduced such that it can share physical stresses but with minimum impact on membrane water uptake and proton conductivity.

This study reports the effect of reduced particle loading on the performance and durability of Nafion® membrane. The goal is to improve membrane durability without significantly sacrificing membrane performance—an optimization approach.

EXPERIMENTAL

Materials

Titanium isopropoxide (Gelest Inc.) and 2,4-pentanedione (Acros organics) were used as received. Extruded Nafion® 112 membranes were received from E.I. Dupont Co.

Membrane cleaning and composite preparation

Nafion® 112 membranes were cleaned by boiling in 8*M* nitric acid for 2 h followed by boiling in deionized water twice for 2 h to leach out residuals. The membranes, after drying at 80°C under vacuum for 24 h, were weighed to measure initial weight. Titanium iso-propoxide $Ti(OiPr)_4$ was used as the sol–gel precursor monomer, and 2,4-pentanedione was added as a complexing agent to reduce the otherwise rapid sol–gel reaction rate. A ratio of 1.5 : 1 for 2,4-pentanedione : $Ti(OiPr)_4$ was maintained. The mole fraction of $Ti(OiPr)_4$ in the reaction mixture was 0.01. The membrane was swollen in methanol for 24 h after which it was temporarily removed for $\sim$ 30 s, during which time the sol–gel precursor monomer and 2,4-pentanedione were added and stirred to form a homogeneous reaction solution. Then, the membrane was reimmersed for 15 min, and after removal from the reaction mixture followed by methanol wash, it was dried at 100°C for 16 h. After drying, the membrane was refluxed in 8*M* HNO_3 for 2 h followed by refluxing in deionized water twice for 1 h each time. The membranes were then dried at 100°C for 24 h under vacuum. A control Nafion® sample was subjected to similar processing conditions.

MEA preparation

MEAs were prepared using Pt/C catalyst for both anode and cathode. Catalyst ink was prepared by mixing 30% HP Pt on Vulcan XC-72 (BASF Fuel Cell Inc.) with a 5 wt % Nafion® solution in a homogenizer for 10 min. The Nafion® content in the electrode was targeted to be 30%. The ink was then

applied on a Teflon sheet by screen printing. After drying, this was then decal transferred to the membrane in a Carver hot press under a pressure of 12 atm at 120°C for 5 min. The platinum loading in the electrode was gravimetrically estimated to be 0.43 + 0.01 mg cm^{-2}. MEAs were assembled in a 5 cm^2 Teledyne Energy Systems fuel cell hardware containing triple-serpentine flow fields. Two 275 μm Toray carbon papers (TGPH-090) were used as gas diffusion layers in the assembly. The assembly was sealed using two 250 μm Teflon gaskets, and a torque of 4.5 N m was applied on all the eight bolts of the assembly.

Inorganic uptake

The difference between the dried membrane weights following the sol–gel treatment and subsequent nitric acid/water cleaning is considered as the titania weight uptake.

Equivalent weight (EW) measurement

Vacuum-dried membranes, after weighing for initial weight, were added to a flask containing deionized water and soaked for 24 h. To neutralize the acidic groups, a known excess of 0.01*N* standard sodium hydroxide solution was added to the flasks and stirred for 3 h. Excess sodium hydroxide was measured by titrating against 0.01*N* standard acetic acid solution using phenolphthalein as indicator. EW was calculated by dividing number of moles of sodium hydroxide consumed by the sample into its dry weight.

FTIR analysis

The nature of chemical bonding in the *in situ*-grown titanate nanostructures was investigated by FTIR/ATR spectroscopy using a Bruker Equinox 55 instrument. Each spectrum represents an average of ten, specifically five on each side of the membrane collected at different locations on the surface. Spectra were baseline corrected and smoothed. The spectra were truncated below 530 cm^{-1} due to considerable noise at lower wave numbers.

Water uptake

Water uptakes for the membranes were precisely measured using a TA instruments Q5000SA Dynamic Vapor Sorption Analyzer. Membranes after equilibration at 80°C were subjected to an RH change from 90 down to 0% in 10% steps. Samples were conditioned at each step for 1 h, and the weight gain toward the end of that step was used to calculate water uptake. Membrane weight at the end of the 0% RH step was considered as dry weight and used to calculate percent water uptake.

Proton conductivity

Proton conductivities were measured using a Bekktech BT-512 conductivity system in a four point probe configuration. The membrane resistance was calculated using a scanning DC technique. A voltage sweep from +0.1 to −0.1 V at steps of 0.01 V was performed and the resultant current across the electrode was measured. The slope of the voltage–current line yields the membrane resistance, R, from which conductivity is calculated using the equation $\sigma = L/(RWT)$, where L is the distance between electrodes and W and T are membrane width and thickness, respectively of dry membrane. The relative humidity at 80°C experienced by the membrane in the conductivity cell was increased in steps of 10% from 20 to 100%. Conductivity during the experiment was continuously measured at intervals of 5 s. At each step, the sample was conditioned for 1 h, and the conductivity toward the end of the step was taken as the proton conductivity for that particular RH.

Mechanical properties

Tensile properties of titania-modified and unmodified membranes at 80°C and 100% RH were tested using an MTS Alliance RT/10 tensile setup equipped with a custom-designed environmental chamber. The same equipment and test setup were used to study the build-up of contractile stresses developed in constrained membranes vs. time following a RH drop. Mechanical properties of MEAs postdegradation were studied using a TA Q800 dynamic mechanical analyzer. Tensile strength and creep response to a 5 MPa stress at 80°C were analyzed without controlling the RH of the sample chamber.

Fuel cell performance and open circuit voltage (OCV) test

Polarization curves were obtained at 80°C with 100% anode and 50% cathode inlet RH. Oxygen was used as oxidant (0.5 slpm), and pure hydrogen was used as fuel (0.2 slpm). The current was scanned from 0 Amperes until the cell voltage dropped below 0.1 V to get enough points in low current (0.01, 0.03, 0.1, 0.15, 0.25, 0.5, 0.75 and 1 Ampere) and high current (2, 2.5, 3, 3.5, 4, 4.5, 5, 5.5, 6, 7, 8, 9, 10, 11, and 12 Ampere) regimes. For each current density, the cell voltage was recorded after 30 s hold time. Before obtaining polarization curves, the membranes were conditioned for 6 h at 0.8 V. All MEAs were tested on a Scribner Associates (Model 850C) fuel cell test station.

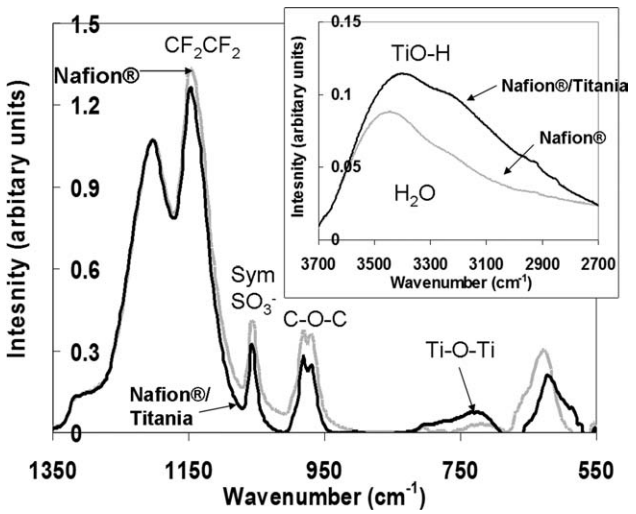

Figure 1 FTIR-ATR spectra of Nafion® and Nafion®/titania membranes.

To test membrane durability, MEAs were run under OCV conditions at 90°C and 30% inlet RH. Ultra high pure hydrogen (at 0.2 cc/min) and ultra high pure oxygen (at 0.2 cc/min) were used as fuels. The test was performed for 48 h at an interval of 24 h. Following every 24 h accelerated OCV degradation, polarization curves were recorded at 80°C at 100% anode and 50% cathode inlet RH. Effluents from anode and cathode cold traps were collected for fluoride analysis after recording polarization curves. Before the test, cold traps and the exhaust pipes were thoroughly washed to ensure no fluoride contaminants were present. Fluoride ion concentrations in the condensate water were measured using a F^- ion selective electrode (Denver instruments), which was calibrated before each measurement.

RESULTS AND DISCUSSION

Inorganic weight uptake

Titania weight uptake for the composite membrane was 12%. The control sample lost 1.2% of its initial weight, due to low-molecular weight fragments being leached out in alcohol solution during membrane swelling. The exact EWs for Nafion® and Nafion®/titania membranes were 1107 and 1122, respectively. This indicates that sol–gel modification has essentially not changed the concentration of acidic groups that are essential for proton transport.

FTIR-ATR analysis

ATR-FTIR spectra of Nafion® and Nafion®/titania membranes are shown in Figure 1. The band assignments for Nafion® are based on the listing by Falk,[20] and assignments for titanates are based on the work of Siuzdak et al.[21] The C—F stretching band at 1200 cm^{-1} was used as an internal standard to scale the absorbance of both the spectra. The absorbance of polymer bands in the composite membrane is lower than that of Nafion® due to the dilution of chemical groups by the inserted titania.[19] The invariance in peak positions and widths for asymmetric S—O stretching in SO_3^- groups at $\sim$ 1200 cm^{-1} as well as symmetric stretching of the SO_3^- group at $\sim$ 1056 cm^{-1} suggests that the incorporated titania network has not altered the molecular environment, nor they are interacting with sulfonic acid groups. This is in harmony with the observed unchanged EW upon titania inclusion. The doublet around 980–960 cm^{-1} for the two ether groups in the side chain is intact, but the intensity of the lower wavenumber component absorbance is reduced relative to the high wavenumber component. This might indicate penetration of titania nanostructures closer to the backbone.

Evidence of successful condensation of titania networks is presence of the Ti—O—Ti stretching vibration at $\sim$ 700 cm^{-1}.[19] The broadness of this peak indicates a broad distribution in molecular environment (varying degrees of Ti atom coordination) about these vibrating groups. Related to this, the inset in the figure shows the absorbance due to O—H stretching vibration for the modified and unmodified membrane. In the case of Nafion®, this band is likely due to hydrogen bonded water, whereas for the dried modified membrane, it can also be due to O—H stretching in Ti(O—H) groups.

Water uptakes for Nafion® and Nafion®/titania membranes at different RH are shown in Figure 2. Uptake for the composite membrane is calculated with respect to the Nafion® fraction (0.88) in the material. The inset in the figure shows the ratio of water uptake for Nafion® to that of Nafion®/titania.

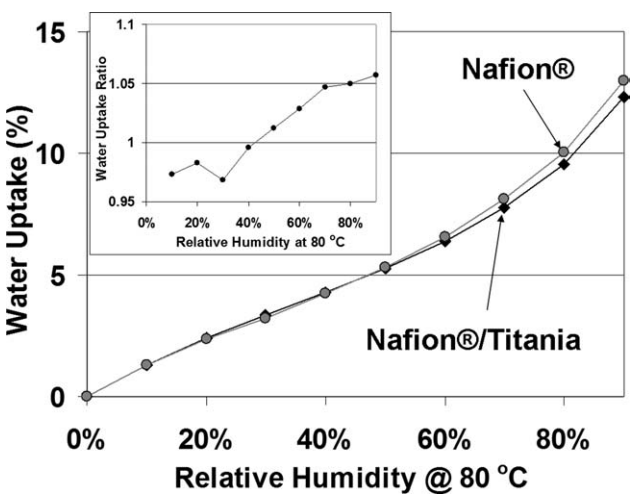

Figure 2 Water uptake of Nafion® and Nafion®/titania membranes at 80°C. Inset: Nafion®: Nafion®/titania water uptake ratio.

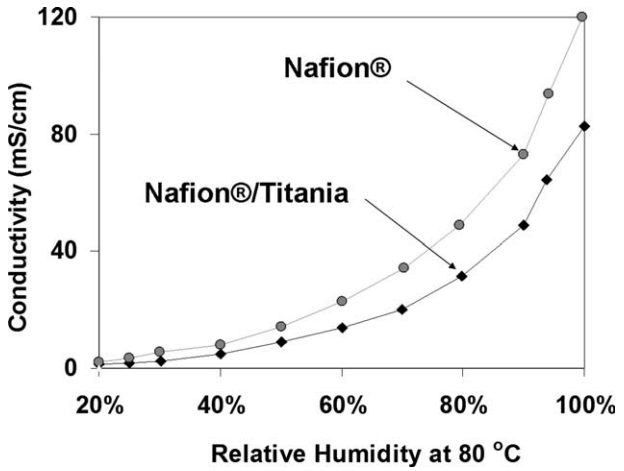

Figure 3 Proton conductivity of Nafion® and Nafion®/titania membranes at 80°C.

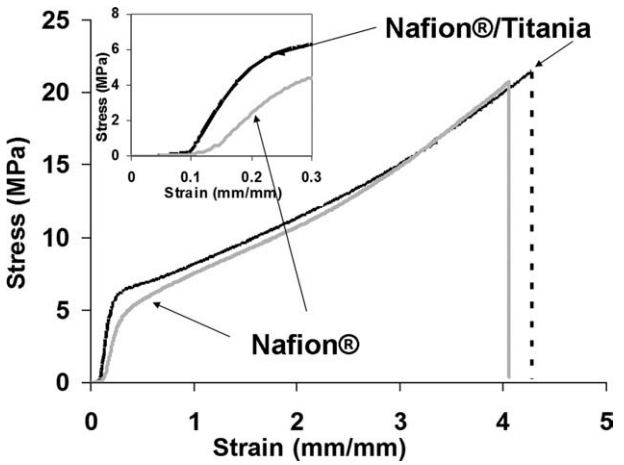

Figure 4 Tensile stress–strain curves at 80°C and 100% RH for Nafion® and Nafion®/titania membranes. Inset is initial strain region.

Nafion® shows slightly higher water uptake at RH > 40%. Restricted polymer swelling as well as the occupancy of volume in the cluster regions by the titania reinforcements reduce free volume available for the water molecules. On the contrary, the impediments for Nafion® water swelling are less, and the volume gain is entirely accounted for by water molecules. At lower RH, the uptake, however, is marginally higher for composite membranes. Perhaps, the difference is negligible and within instrumental error limits, but addition of inorganic particles have been reported to improve water uptake at lower RH.[22] These particles have uncondensed surface hydroxyl groups that can bind water through hydrogen bonds and retain water at lower water activities.

Proton conductivity

Proton conductivities of Nafion® and Nafion®/titania membranes at various RH at 80°C are plotted in Figure 3. As expected, the conductivity of Nafion®/titania is lower than that of unmodified Nafion® at all RH. Although titania reinforcement does not alter effective EW, it has lowered water uptake that reduces proton conductivity. Another reason for lower conductivity could be reduced conformational flexibility of side chains as they may become embedded in the inorganic phase during the sol–gel reaction. While the SO_3H groups remain accessible, it appears that something is interacting with one of the ether oxygen atoms in the side chains. This would hinder proton hopping between SO_3H groups.

Conductivity σ is not a pure, but rather a compound quantity that depends on both charge carrier density ρ and mobility μ by the equation $\sigma = \rho\mu$. σ can decrease with decrease in ρ owing to the dilution of SO_3H groups by titania insertion, but it can also decrease due to a reduction in μ due to reduced water uptake, reduced side chain mobility and increased proton migration tortuosity.

Mechanical properties

Figure 4 is a representative of stress–strain curve for Nafion® and a Nafion®/titania composite membranes at fuel cell operating conditions. Membranes after conditioning for 2 h at 80°C and 100% RH in a custom-designed environmental chamber were stretched at 5 mm/min to their strain-at-break. The initial horizontal strain displacement with no stress is due to sample expansion on swelling during conditioning, and the load cell does not register force until the sample reaches its natural length. This curve displacement measures sample dimensional change. After this, the curve is typical of a ductile material from which mechanical properties can be computed. The inset in the figure shows maximum

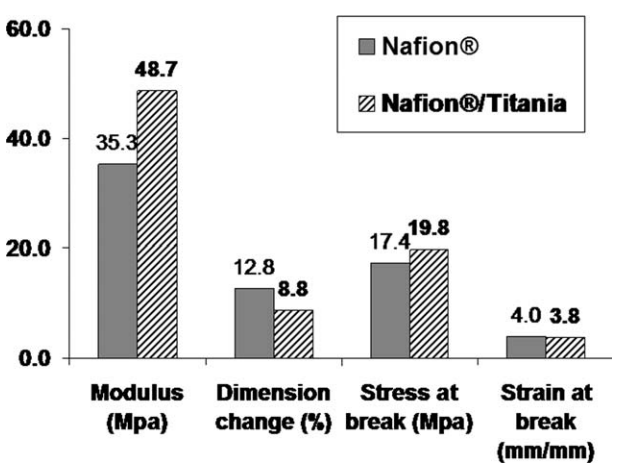

Figure 5 Tensile properties at 80°C and 100% RH for Nafion® and Nafion®/titania membranes.

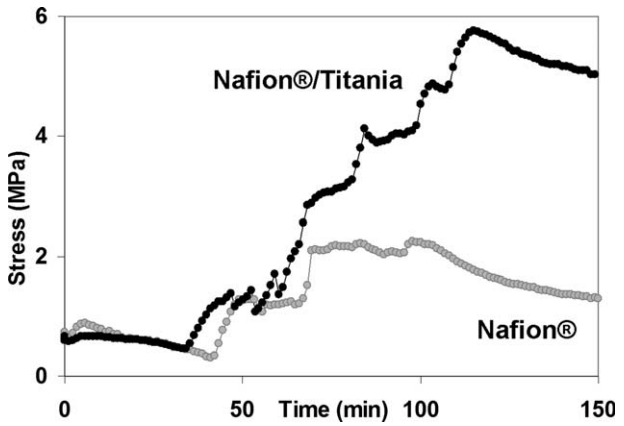

Figure 6 Contractile stress response to RH drop from 100 to 0% at 80°C for Nafion® and Nafion®/titania membranes.

strain up to the displacement when stress begins to rise which is the percent increase in sample length from the dry state due to water uptake. The composite membrane, on account of swelling restriction due to particle reinforcement, imparts better dimensional stability. Figure 5 summarizes average mechanical properties of Nafion® and Nafion®/titania membranes. Titania incorporation increased the modulus by 40% and reduced swelling by 30%, and there is slightly improved stress-at-break. This change may not appear significant compared to our previous reported modification involving higher titania loading.[19] In particular, for 20% titania incorporation, the modulus increased by 230% although the membrane showed poor fuel cell performance.

Figure 6 shows contractile stresses developed at 80°C by Nafion® and Nafion®/titania membranes subjected to an RH drop from 100 to 0%. Membranes after clamping in the tensile setup were conditioned for 2 h with an 80°C, 100% RH nitrogen stream supplied at 300 cc/min. After conditioning, to hold the membrane at its extended swollen length due to water uptake, the crosshead position was slowly adjusted until a tension of 0.1*N* was detected by the load cell. The crosshead position was then locked and the 100% humidified stream was switched to 300 cc/min, 0% RH nitrogen at 80°C. The dry stream caused the membrane to lose water causing the membrane attempt to contract to its unswollen length except that the sample, being clamped at fixed positions, consequently exerts contractile stress, which is monitored vs. time.

Both modified and unmodified membranes eventually yield by chain slippage through chain entanglements. The modified membrane offers better resistance to deformation and yields after 5.8 MPa, whereas unmodified Nafion® yields after only 2.2 MPa. The modified membrane, with higher modulus due to reinforcement, offers better resistance to deformation and yields at a higher stress. This behavior is different from our previous study where a membrane containing the greater quantity of 20% titania maintained a constant stress of 9 MPa without yielding during drying. For higher titania loading, the inorganic structures may have formed an interknitted load-bearing network and prevented membrane yielding or simply "cemented" chains together. However, for lower titania loading, the reinforcements are isolated and share stresses with the matrix. The reinforcement improves the ability to withstand stresses associated with temperature and humidity changes in a fuel cell. Without such reinforcement, the unmodified membrane will experience structural and mechanical hysteresis such that swelling fatigue eventually causes local yielding leading to cracking and failure.

OCV test

Figure 7 shows 48 h OCV curves for both Nafion® and Nafion®/titania membranes in a fuel cell at 90°C and 30% inlet relative humidity's. In both cases, the experiment was stopped after 24 h to collect anode and cathode effluent for fluoride analysis and to generate performance curves. The high OCV value at the start of experiment for the composite membrane, 0.99 V, indicates a better gas barrier property than that of Nafion® at 0.92 V. In 48 h, although the voltage drop is not linear, Nafion® lost 0.41 V at a rate of 8.5 mV/h, whereas Nafion®/titania lost only 0.14 V at 2.9 mV/h. Throughout the course of the experiment, OCV for the composite not only stayed higher but also decayed at a much lower rate, which is attributed to better dimensional stability and improved mechanical and gas barrier properties. The reinforcement adds gas diffusion tortuosity that restricts membrane degradation and OCV loss due to reduced fuel crossover.

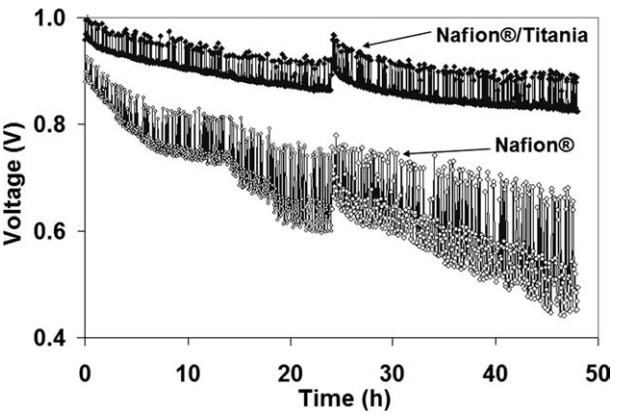

Figure 7 OCV curves for Nafion® and Nafion®/titania membranes at 90°C and 30% RH.

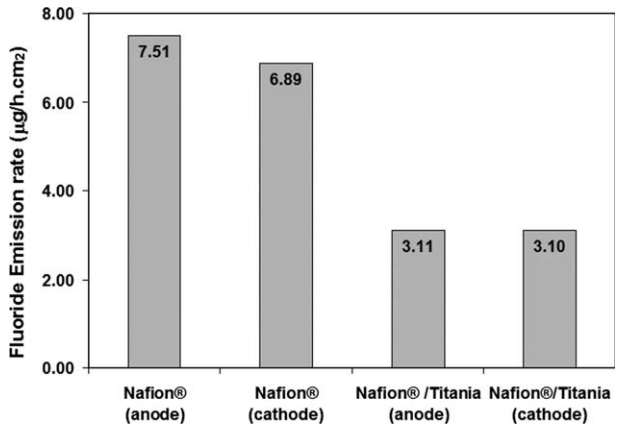

Figure 8 Fluoride emission rates of Nafion® and Nafion®/titania composite membranes for anode and cathode after 48 h of OCV test at 90°C 30% RH.

Fluoride emission rate (FER)

The cumulative fluoride contents of anode and cathode effluents after 48 h of OCV testing are shown in Figure 8. The FER for the composite membrane is less than half that of Nafion® for both anode and cathode. This reflects a reduced rate of chemical degradation due to the titania reinforcement which introduced tortuosity for fuel molecules in their drive to reach opposite electrodes. Reduced fuel crossover retards the rate of peroxide formation, which lowers chemical degradation of the membrane, that will not only prolong membrane life but would also be less wasteful of fuel due to improved gas barrier properties.

Fuel cell performance

Figure 9 shows fuel cell performance curves for Nafion® and Nafion®/titania membranes before and after 48 h the OCV test. Considering the lower water uptake and lower proton conductivity of the composite membrane, its performance curve was expected to be lower than that for the Nafion® membrane.

The primary focus of this work was to improve the important property of membrane durability without significantly sacrificing fuel cell performance. Both before and after OCV degradation, the performance of the Nafion® membrane is better than that of composite membrane. However, performance deterioration post-OCV degradation is higher for Nafion®. The inset in Figure 9 compares the initial part of the performance curves. The starting voltage at zero current for Nafion® decreased from 0.92 to 0.74 V. At low current densities, the performance of the composite membrane is better than Nafion®. The inferior performance at low current densities for unmodified Nafion® is due to increased fuel cross over due to high membrane degradation. The inability to withstand physical stresses severely degraded the membrane and pathways for fuel cross over were created. This will not only degrade the membrane faster, reducing the life of the fuel cell but also would make it less efficient due to the voltage penalty associated with fuel crossover. The improved mechanical and barrier properties of the composite membrane enabled it to better withstand accelerated degradation. The starting voltage at zero current only decreased from 0.98 to 0.95 V. Also, the relative displacement of the performance curve post-degradation is low indicating that the membrane still has better barrier properties and, assumedly, formed fewer pathways for gas crossover.

One can quantitatively compare the performance loss of the two membranes following degradation by comparing the area under the power curves. Figure 10 shows the power curves for Nafion® and Nafion®/titania membranes before and after 48 h of

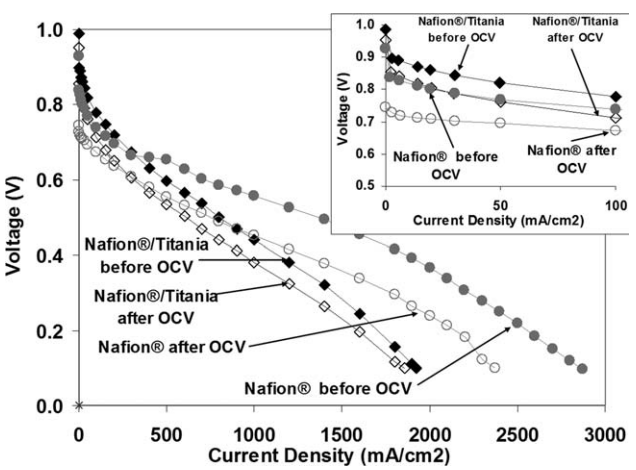

Figure 9 Polarization curves for Nafion® and Nafion®/titania membranes before and after OCV conditions at 80°C; anode at 100% RH and cathode at 50% RH.

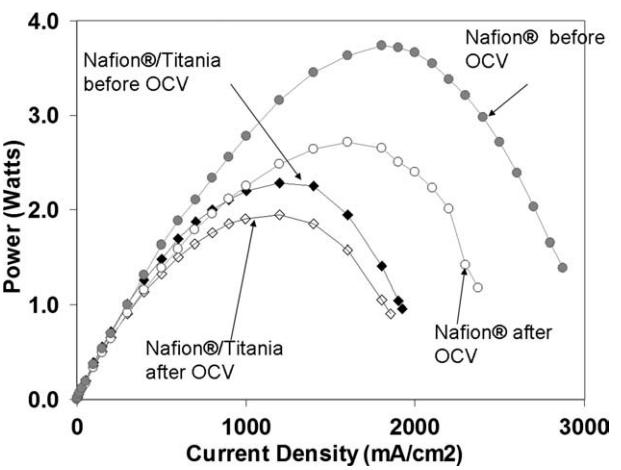

Figure 10 Power curves for Nafion® and Nafion®/titania membranes before and after OCV conditions at 80°C; anode at 100% RH and cathode at 50% RH.

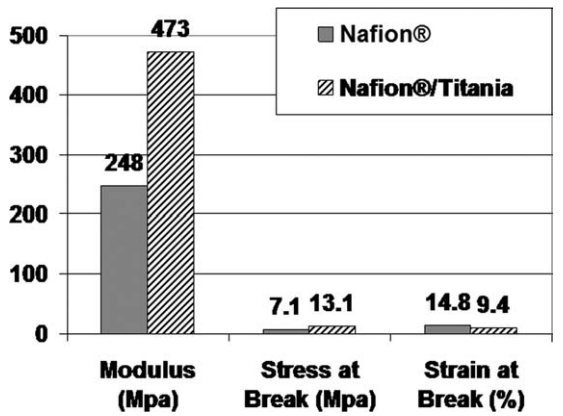

Figure 11 Tensile properties of Nafion® and Nafion®/titania degraded MEAs at 80°C after the OCV test.

OCV testing. The area calculated under the power curves for Nafion® before and after degradation is 650 and 430, respectively, whereas that of composite membrane before and after degradation is 410 and 345, respectively. After degradation, the decrease in the area under the power curve with respect to the initial power curve for Nafion® is 34% whereas that of composite membrane, it is only 15%. This suggests that the Nafion® membrane, while performing better in the beginning, has a higher voltage loss due to fuel cross over and will be less efficient over time. The ratio of the area under the power curves of the composite membrane to Nafion® before and after degradation is 0.63 and 0.80, respectively. Perhaps, with further development, the performance of the composite membrane may match or exceed that of Nafion® with an added benefit of longer membrane life and efficient fuel utilization. Also, if operated at lower current densities, the performance difference would be negligible.

Mechanical properties of degraded MEAs

After OCV degradation test, the tensile properties of the MEAs were measured in a dynamic mechanical analyzer at 80°C without humidity control. The average mechanical properties for three randomly selected samples taken from different locations of the same degraded MEAs for Nafion® and Nafion®/titania composite membranes are shown in Figure 11. The modulus and the stress-at-break for the composite MEA is almost twice that of Nafion® that indicates that the composite can better withstand stresses, is less likely to yield and can survive longer in the fuel cell. Strain-at-break, however, is lower, which is not surprising considering the reinforcement.

Creep tests were performed on degraded MEAs to check their deformation response to constant load. In an actual fuel cell, the stress profile associated with temperature, humidity, and current change will be complex, to be sure. In the interest of rapid screening, a simple comparison was done by subjecting degraded MEAs to a constant stress at 80°C. Samples, after being equilibrated at 80°C for 2 min, were subjected to a constant stress of 2 MPa and 5 MPa for 3 h. The resulting strain was monitored during and after (release) application of stress for 3 h in each case. Figure 12(a) shows strain responses for degraded Nafion® and Nafion®/titania MEAs subjected to 2 MPA stress. The unmodified Nafion® MEA deformed by 3.7% out of which 45% recovered after stress removal. Nafion® membranes have been reported to significantly reduce their ductility when subjected to the OCV degradation test. During deformation, the polymer chains slip by each other and through entanglements, and the low modulus is insufficient to resist deformation. This structural deterioration will cause membrane thinning and introduce weak regions that offer less resistance to fuel crossover. After degradation, due to reduced ductility, the applied stress may generate microscopic cavities rather than crazes that are spanned by fibrils. The composite MEA deformed by 0.9% of

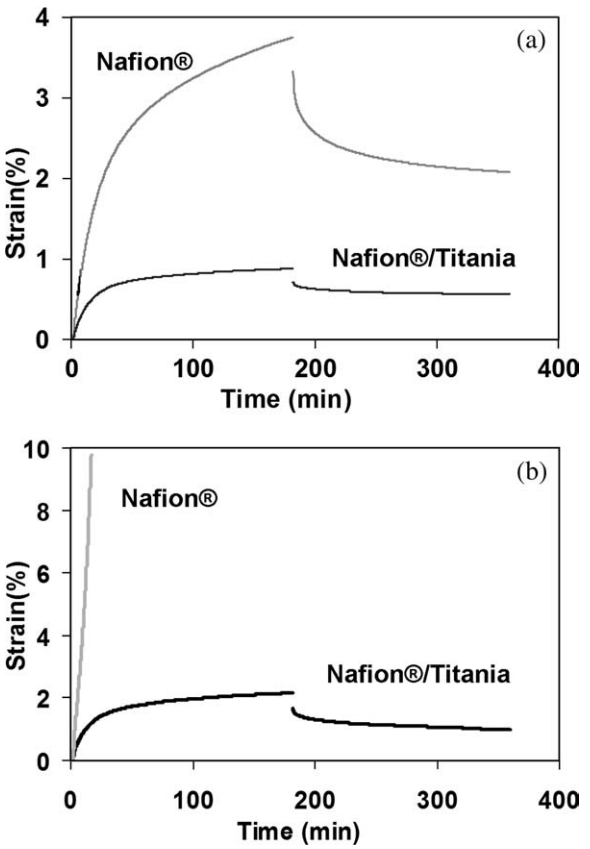

Figure 12 (a) Creep response of Nafion® and Nafion®/titania degraded MEAs to a constant 2 MPa stress at 80°C after the OCV test and (b) Creep response of Nafion® and Nafion®/titania degraded MEAs to a constant 5 MPa stress at 80°C after the OCV test.

which 36% is recovered after removal of stress. While the strain recovery of the degraded composite membrane is less, the overall permanent deformation is lower than that of Nafion® which suggests fewer weak spots are formed which would facilitate gas crossover.

Figure 12(b) shows the strain response for Nafion® and Nafion®/titania degraded MEAs subjected to a constant 5 MPA stress. It is observed that within 16 min of stress application, the Nafion® MEA deformed by 9.5% and ruptured. However, the composite MEA withstood during the entire test and deformed only by 2.2% of which 55% was recovered after stress removal. This result agrees with the mechanical test results of the degraded MEAs confirming that the composite membrane can handle stress better and is more likely to be more durable in a fuel cell.

CONCLUSIONS

Titania particles were incorporated in Nafion® membranes via polymer-*in situ* sol–gel reactions. Evidence of successful Ti—O—Ti intraparticle bonds and uncondensed hydrophilic TiOH groups was provided by FTIR spectroscopy. This inorganic modification did not alter membrane EW as shown by titration and inferred by FTIR spectroscopy. Vapor pressure isotherms showed that water uptake of the composite was essentially identical to that of the unmodified control at less than 50% RH and only slightly lower at higher RH. Observed increased tensile modulus with this reinforcement contributed to dimensional stability against humidity change. Contractile stress buildup, during drying from a swollen state, of a sample clamped at constant length, demonstrated considerable reinforcement of Nafion® by these titania inclusions. Although the modification enhanced mechanical properties, proton conductivity and fuel cell performance were diminished. OCV tests showed that the reinforcement minimized voltage loss and reduced chemical degradation due to improved gas barrier properties. FER for the composite membrane is less than half that of Nafion® for both anode and cathode. After an accelerated OCV test, the fuel cell performance of the modified membrane lowered slightly, whereas that of the unmodified membrane deteriorated significantly and was lower than that of the modified membrane at low current densities. The performance drop for the unmodified membrane was attributed to increased fuel crossover where gas migration pathways were enhanced during the OCV test. The view is that the unmodified membrane is unable to withstand stresses due to humidity change in a reactive radical environment and fails. The reinforcement lowers formation of radical species by reducing fuel crossover and shares physical stresses which prevent membrane failure and formation of crossover pathways. The failure of an OCV-degraded MEA during tensile creep testing draws attention to the importance of mechanical integrity for membrane durability.

Relative to our earlier studies involving similar titania-modified Nafion® membranes, the reduced inorganic content in the samples reported here appears to be a step toward balancing fuel cell performance against durability. Particle incorporation reduces free volume for water to occupy and restricts side chain mobility although proton conductivity and fuel cell performance is lowered. Poor dimensional stability in unmodified membranes is caused by excessive swelling, while greater hydration in the sulfonic acid domains promotes good proton mobility. Differential swelling stresses during humidity and temperature cycling causes mechanical hysteresis that generates additional free volume that can enhance pathways for fuel crossover which, in turn, generates more free radicals that accelerate chemical degradation. The same structure and properties that cause good Nafion® membrane performance at less than 100°C also lead to its failure. Well-dispersed inorganic particles decrease fuel crossover by increased tortuosity and dimensional stability is enhanced as the ability to withstand stresses associated with temperature and humidity change is improved. Thus, this simple modification retards both physical and chemical degradation, which are coupled.

This modification will extend membrane lifetime and waste less fuel due to decreased gas permeation. In the future, perhaps the limitation of low proton conductivity can be overcome by attaching acid moieties on $[Ti(O_{1/2})_4]_X(OH)_y$ particle surfaces through reactions with free Ti—OH groups. This modification might also allow the use of membranes with lower EW which, thus far, have been found to be unsuitable due to poor water stability.

The authors thank DuPont Co. for Nafion® samples. The authors also thank Prof. Vijay Ramanai and Panagiotis Trogadas for their help in the fluoride analysis of chemical degradation.

References

1. Souzy, R.; Ameduri, B. Prog Polym Sci 2005, 30, 644.
2. Crum, M.; Liu, W. ECS Trans 2006, 3, 541.
3. Liu, W.; Ruth, K.; Rusch, G. J N Mater Electrochem Syst 2001, 4, 227.
4. Bauer, F.; Denneler, S.; Willert-Porada, M. J Polym Sci Part B: Polym Phys 2005, 43, 786.
5. Patil, Y. P.; Seery, T. A. P.; Shaw, M. T.; Parnas, R. S. Ind Eng Chem Res 2005, 44, 6141.
6. Inaba, M.; Yamada, H.; Tokunaga, J.; Tasaka, A. Electrochem Solid State Lett 2004, 7, A474.
7. Liu, W.; Zuckerbrod, D. J Electrochem Soc 2005, 152, A1165.

8. Teranishi, K.; Kawata, K.; Tsushima, S.; Hirai, S. Electrochem Solid State Lett 2006, 9, A475.
9. Madden, T.; Weiss, D.; Cipollini, N.; Condit, D.; Gummalla, M.; Burlatsky, S.; Atrazhev, V. J Electrochem Soc 2009, 156, B657.
10. Mittal, V. O.; Kunz, H. R.; Fenton, J. M. J Electrochem Soc 2006, 153, A1755.
11. Aoki, M.; Uchida, H.; Watanabe, M. Electrochem Commun 2005, 7, 1434.
12. Curtin, D. E.; Lousenberg, R. D.; Henry, T. J.; Tangeman, P. C.; Tisack, M. E. J Power Sources 2004, 131, 41.
13. Zhou, C.; Guerra, M. A.; Qiu, Z.-M.; Zawodzinski, T. A.; Schiraldi, D. A. Macromolecules 2007, 40, 8695.
14. Escobedo, G. Fuel Cells Durability, 1st ed.; Knowledge Press: Brookline, MA; 2006. p 83.
15. Thompson, E. L.; Jorne, J.; Gasteiger, H. A. J Electrochem Soc 2007, 154, B783.
16. Inaba, M.; Kinumoto, T.; Kiriake, M.; Umebayashi, R.; Tasaka, A.; Ogumi, Z. Electrochim Acta 2006, 51, 5746.
17. Mauritz, K. A.; Hassan, M. K. Polym Rev 2007, 47, 543.
18. Mauritz, K. A.; Stefanithis, I. D.; Davis, S. V.; Scheetz, R. W.; Pope, R. K.; Wilkes, G. L.; Huang, H.-H. J Appl Polym Sci 1995, 55, 181.
19. Patil, Y. P.; Mauritz, K. A. J Appl Polym Sci 2009, 113, 3269.
20. Falk, M. ACS Symp Ser 1982, 180, 139.
21. Siuzdak, D. A.; Start, P. R.; Mauritz, K. A. J Polym Sci Part B: Polym Phys 2002, 41, 11.
22. Jalani, N. H.; Dunn, K.; Datta, R. Electrochim Acta Electrochim Acta 2005, 51, 553.